

High-efficiency biomass gasifier SOFC systems with direct internal tar reforming

Cavalli, A.; Aravind, P. V.

DOI

[10.1149/09101.0781ecst](https://doi.org/10.1149/09101.0781ecst)

Publication date

2019

Document Version

Accepted author manuscript

Published in

ECS Transactions

Citation (APA)

Cavalli, A., & Aravind, P. V. (2019). High-efficiency biomass gasifier SOFC systems with direct internal tar reforming. *ECS Transactions*, 91(1), 781-790. <https://doi.org/10.1149/09101.0781ecst>

Important note

To cite this publication, please use the final published version (if applicable).
Please check the document version above.

Copyright

Other than for strictly personal use, it is not permitted to download, forward or distribute the text or part of it, without the consent of the author(s) and/or copyright holder(s), unless the work is under an open content license such as Creative Commons.

Takedown policy

Please contact us and provide details if you believe this document breaches copyrights.
We will remove access to the work immediately and investigate your claim.

High-Efficiency Biomass Gasifier SOFC Systems with Direct Internal Tar Reforming

A. Cavalli^a, P. V. Aravind^a

^a Process & Energy Department, Technical University of Delft, Delft, The Netherlands

Removing biosyngas contaminants is crucial for the efficient and safe operation of biomass gasifier solid oxide fuel cells systems. Among the contaminants, tar might be considered an additional fuel if converted into H₂ and CO in a reformer or directly in the SOFC. However, no sufficient information is available on direct internal tar reforming. The knowledge gained during the 4-years project FlexiFuel-SOFC is presented. The aim of these studies was to determine the possibility to directly reform tar in the SOFC, and to assess the influence that other biosyngas contaminants (i.e., H₂S and HCl) can have on the process. Benzene can be regarded as fuel, while naphthalene as a contaminant. Also toluene can be reformed inside the SOFC, but HCl seems to affect the process. Acetic acid is completely converted inside SOFCs and its conversion appears not affected by H₂S. However, it causes carbon deposition, mainly in the inlet pipelines.

Introduction

Biomass gasifier solid oxide fuel cells systems are an alternative to fossil fuel based power and heat generation systems. In these systems, the solid biomass is converted into a gaseous mixture called biosyngas, mainly composed of hydrogen, carbon monoxide, methane, carbon dioxide, nitrogen, and steam. Other compounds are present in lower concentrations: sulphur, halides, particulate matter, and tar compounds. These species are harmful for downstream equipment and are therefore removed in the system gas cleaning unit (GCU) operating at low or high temperature (> 300 °C). Gas cleaning is a crucial step in the system heat management, and it affects the system complexity and overall efficiency.

Tar compounds, together with light condensable and volatile organic compounds, play a fundamental role among biosyngas contaminants. In low temperature GCUs, these compounds are removed from the gas. Differently, in high temperature GCUs, they are converted into H₂ and CO via endothermic steam and/or carbon dioxide reforming. The heat required for these reactions can be provided by partial oxidation, or by the SOFC flue gas, either via heat exchangers or anode gas recirculation. However, reforming might take place directly inside the SOFC due to the presence of Ni catalyst, steam and carbon dioxide, and the SOFC operating temperature. The heat required is provided directly by the exothermic operation of the SOFC. The endothermic reforming reactions therefore cool down the SOFC, thus decreasing the excess air commonly used to maintain constant the SOFC temperature. The direct internal reforming of these compounds, hereinafter generally named tar, simplifies the system by removing the tar removal stage in the GCU and the required heat management network. Moreover, it might increase overall

efficiency due to the use of the tar energy content and the lower excess air required to cool down the SOFC.

Nonetheless, direct internal tar reforming might cause performance losses due to carbon deposition and even irreversibly damage the cell due to thermal and mechanical stress (1). Liu et al. observed carbon deposition on a Ni-YSZ cell fed with biosyngas containing 6.3 g/Nm³ toluene (2). Papurello et al. found a large decrease in the performance of a Ni-YSZ cell fed with biosyngas when only 0.1 g/Nm³ toluene were present (3,4). Namioka et al. defined a tolerance limit of 3 g/Nm³ toluene in humidified hydrogen for a Ni-ScSZ SOFC operating at 800 °C and 500 mA/cm². The authors did not observe any carbon deposition, but SEM-EDS analysis indicated disappearance of Ni particles (5). However, other authors defined higher tolerance limits. As an example, Madi et al. observed no significant added degradation of a Ni-YSZ cell with up to 4.1 g/Nm³ toluene on dry H₂, and even up to 14.4 g/Nm³ on biosyngas (6). Also Baldinelli et al. tested Ni-YSZ cells with 10 g/Nm³ toluene in biosyngas and no carbon was observed in post-mortem analysis (7). Ni-GDC cells are reported to have even higher tolerance limits. Liu et al. obtained no degradation with 20 g/Nm³ toluene in biosyngas (8). Doyle et al. observed carbon deposition with SEM-EDS analysis, but 20 g/Nm³ toluene actually increased the cell performance by decreasing the cell ASR and increasing the amount of fuel available due to the tar reforming. Nonetheless, 32 g/Nm³ dramatically affected the ASR (9). Other studies have used naphthalene (10–12) and benzene (13,14). Aravind et al. showed that few ppm of naphthalene are tolerated by Ni-GDC anodes (12). However, the presence of the contaminant hinders the reforming of methane (11). Also Papurello et al. suggested that for Ni-YSZ anode supported cells, while light tar as benzene and toluene can be regarded as fuel, heavy tar as naphthalene must be regarded as a poison (10). The effect of real tar mixtures has also been investigated (15–18). Hofmann et al. obtained a stable performance feeding a Ni-GDC cell with biosyngas containing 10 g/Nm³ tar from a circulating fluidized bed biomass gasifier (17). Nonetheless, while the cell electrochemical performance might appear unaffected, carbon deposition on the anode and on the current collector inside a stack can increase the pressure drop over the stack (19). Moreover, other biosyngas contaminants, such as HCl and H₂S, can affect the reforming reactions occurring in the anode chamber. Excluding the studies of Sasaki et al. on co-poisoning of H₂S and hydrocarbons (20), Papurello et al. (3) and Boldrin et al. (21) on cross influence of sulfur and toluene, the effect of H₂S on tar reforming has not been sufficiently investigated. The same holds for the cross influence of HCl and tar, with exception for a previous work where toluene was used as tar (22).

Direct internal tar reforming can increase overall efficiency and reduce system complexity. Therefore, it can facilitate the development of Integrated Biomass Gasifier SOFC Systems, especially at small scale, which is preferable due to biomass low energy density and scattered distribution. However, SOFC tolerance limits to tar are not yet well defined, and the simultaneous presence of tar and other biosyngas contaminants has to be further investigated. With this background, the knowledge gained during the 4-years project “FlexiFuel-SOFC” is presented in this work. The project aims at developing a highly efficient and fuel flexible micro-scale biomass CHP technology based on a biomass updraft gasifier integrated with an SOFC system (23). Within the project, TU Delft is responsible for the development of a compact gas cleaning concept to remove particles, H₂S, HCl and reform tar compounds. The goal of the investigation was to determine the possibility to directly reform tar inside the SOFC thus avoiding the need of

an external reformer, and to assess the influence that other biosyngas contaminants (i.e., H₂S and HCl) might have on the process. The results are expected to contribute to the further development of this technology.

Methodology

A series of experiments was performed during the project. They can be divided in three groups:

1. Effect of benzene and naphthalene in simulated biosyngas on Ni-GDC cells;
2. Effect of HCl and toluene in humidified H₂-N₂ mixture on Ni-GDC cells;
3. Effect of H₂S and acetic acid in simulated biosyngas on Ni-GDC cells.

In group 1 tests, a ceramic housing (TrueXessory-HT by Horiba-FuelCon) with platinum gauzes as current collector on the cathode side and nickel gauzes on the anode side was used. The anode side current collector had an additional Inconel block, and Inconel rod that was also used for the mechanical load. No additional sealing was required with the housing, and a load of 100 N was sufficient to seal the anode chamber, and assure contact between electrodes and current collectors. Steam was added to the fuel gas stream using a Controlled Evaporator Mixer (CEM) (Bronkhorst, The Netherlands). To add benzene and toluene, a fraction of the dry hydrogen mass flow was bubbled in a temperature controlled bath (tar evaporator). The tar concentration was calculated according to Antoine's equation. Simulated biosyngas (35% H₂O, 2% CO, 20% CO₂, 4% CH₄, 24% H₂ and 16% N₂) with different concentrations of benzene (3 – 15 g/Nm³ d.b.) and naphthalene (0.2 – 0.7 g/Nm³ d.b.) was fed to a Ni-GDC cell operating at 830 °C and 94 mA/cm². Each tar concentration was maintained for 24 hours. The tar effects were evaluated by monitoring the cell operating voltage and with polarization curves recorded using an external load PLZ603W (Kikusui Electronics Corp., Japan) and a DC power supply SM120–25D (Delta Elektronika B.V., The Netherlands). The polarization curves were recorded after two hours from the addition of the tar and at the end of the exposure time; the current was varied only between 0 A (Open Circuit) and the operating current kept during the contaminant exposure. Electrolyte supported cells of 5x5 cm² with an active electrode area of 4x4 cm² with Ni-GDC anode, LSM mixed with ScSZ cathode, and 10Sc1CeSZ electrolyte were used. The outlet gas composition was also analyzed to understand the fate of the tar in the anode chamber. This was monitored using a microGC Agilent 490 with a CP-COX column for measuring CO, H₂, N₂, CH₄ and CO₂ (Agilent, USA). The gas was first passed through a silica-gel desiccator to remove the moisture. The anode outlet flow rate was back-calculated from the inlet N₂ flow rate and the N₂ outlet concentration measured with the microGC. This was then used to calculate the flow rates of H₂, CO, CO₂ and CH₄.

The setups and methodology followed in group 2 and 3 tests have been already described in detail in (22) and (24). Therefore, only a brief description of the testing procedure and conditions is given here. In group 2, a mixture of humidified hydrogen and nitrogen was used as fuel gas to better evaluate the possible changes in the outlet amount of carbon containing compounds due to the simultaneous presence of toluene and HCl. A polarization curve was recorded two minutes after the addition of the contaminant and after 30 minutes of exposure to each HCl concentration (8, 42, 82 ppmv). The procedure was run maintaining the cell at OCV first, and then under a current of 80 mA/cm². The

same approach was followed with toluene alone (2.5, 4.2 and 8.4 g/Nm³), and toluene plus an increasing HCl content (8.4 g/Nm³ plus 2.5, 4.2 and 8.4 g/Nm³). The exposure time was extended to 60 minutes, and the tests were done first with the cell under current and successively with the cell at OCV. All the tests were done on a single 10x10 cm² electrolyte supported cell (ESC) with Ni-GDC anode, LSM mixed with 8YSZ cathode, and 8YSZ electrolyte. The gas composition at the cell outlet was monitored for the whole duration of the experiments.

In group 3, the tar and H₂S were added to simulated biosyngas instead of hydrogen mixture since the contaminants might compete with other compounds (e.g., carbon monoxide and methane) for anode active sites, and therefore the effects observed are more representative of real operation. Two cells of the same type as in group 2 tests were used, one to study the effect of tar alone, and one to test the effect of H₂S first and then the cross-influence of H₂S and acetic acid. The H₂S concentration tested were 0.8 and 1.3 ppmv dry basis, while the concentration of acetic acid was varied from 17 to 128 g/Nm³ dry basis, which is roughly the expected tar amount from updraft gasification (25). To test the cross-influence of acetic acid and H₂S, the cell was first exposed to 42 g/Nm³ acetic acid, then also 0.8 ppmv H₂S were added. Each contaminant concentration was maintained for 24 hours with the cell operated at 68 mA/cm². The outlet gas composition was measured continuously during the tests; polarization curves were recorded with clean biosyngas, and at the beginning and at the end of the exposure to each contaminant concentration. The amount of acetic acid at the cell outlet was measured at the beginning and at the end of the tar injection period by bubbling the gas in two impinger bottles containing isopropanol at room temperature and at 0 °C. Table I summarizes the details of the three groups of experiments performed.

TABLE I. Summary of the most relevant experimental parameters in the three group of experiments.

Group	Cell size and type	Gas flowrates and composition	Contaminants concentration	Operating conditions	Exposure time
1	5x5 cm ² Ni-GDC ESC	A: 1000 NmL/min (35% H ₂ O, 2% CO, 20% CO ₂ , 4% CH ₄ , 24% H ₂ , 16% N ₂) C: 2000 NmL/min (air)	Benzene: 3, 6, 9, 12, 15 g/Nm ³ d.b. Naphthalene: 0.2, 0.7 g/Nm ³ d.b.	830 °C 94 mA/cm ²	24 hours
2	10x10 cm ² Ni-GDC ESC	A: 1400 NmL/min (33% H ₂ , 4% H ₂ O, 63% N ₂) C: 1800 NmL/min (air)	HCl: 8, 42, 82 ppmv Toluene: 2.5, 4.2 and 8.4 g/Nm ³	750 °C 80 mA/cm ²	HCl 30 min; Toluene 60 min
3	10x10 cm ² Ni-GDC ESC	A: 1584 NmL/min (9% H ₂ , 13% CO, 9% CO ₂ , 1% CH ₄ , 30% N ₂ , 37% H ₂ O) C: 3000 NmL/min (air)	H ₂ S: 0.8, 1.3 ppmv d.b. Acetic acid: 17, 41, 83, 128 g/Nm ³	800 °C 68 mA/cm ²	24 hours

Results and discussion

Group 1 experiments

After having reduced the cell at 930 °C by stepwise replacing with H₂ the N₂ anode flow rate used to heat up the setup, the temperature was lowered to obtain a cell temperature of 830 °C. At this temperature, the biosyngas composition tested resulted in a cell OCV of 0.910 V. A polarization curve was measured to verify the proper operation of the cell. Unfortunately, the thickness of the Pt gauzes was not sufficient to assure

proper contact between the current collector on the cathode side and the electrode, and therefore the cell Area Specific Resistance (ASR) was significantly higher than expected (26). As a consequence, the target operating point of 650 mA/cm² could not be reached. The experiments were therefore performed with 98 mA/cm² in order to maintain the operating voltage above 0.8 V. The tests performed at lower current density are anyhow expected to provide useful insights on the tar behavior. In fact, tar can cause carbon deposition on the anode which might decrease the cell ASR due to better contact between the electrode and the current collector, or increase the ASR due to blocking of active sites and gas diffusion channels. The formation of carbon fibers from the Ni grain might also lead to metal dusting. These phenomena are expected to be observable even with lower current density. The cell was kept operating for 100 hours under simulated biosyngas and a new polarization curve was measured to assure no degradation of the cell. Figure 1 shows the two polarization curves recorded at the beginning and after 100 hours operation.

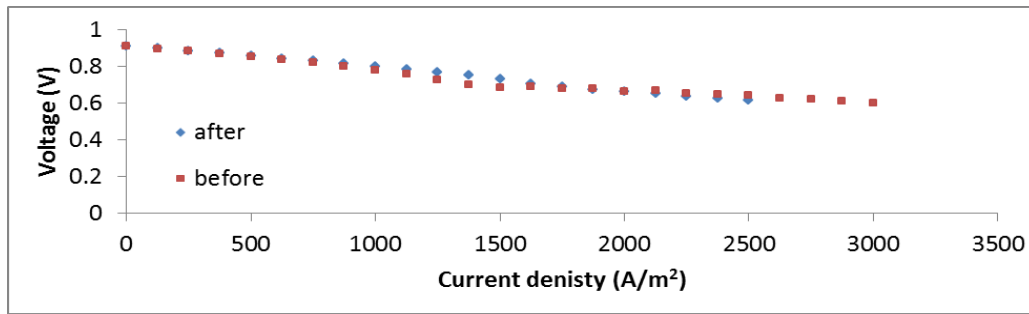


Figure 1. Polarization curves measured at the beginning and after 100 hours operation with simulated biosyngas at 830 °C, 94 mA/cm².

Benzene. With all the tested concentrations, the cell showed no signs of degradation. The voltage increased when benzene was present and, the higher the benzene content, the higher the increase. After this initial increase, the operating voltage remained stable during the exposure time, as visible in Figure 2. The two voltage peaks in the figure corresponds to the two polarization curves, while the single scattered points are measurement inaccuracies due to the device used for logging the voltage and can therefore be neglected. It appears that benzene is reformed inside the cell without negatively affecting the cell electrochemical performance. The cell operating voltage returned to its initial value when the tar flow was stopped. Also the gas composition measured at the outlet showed an increase mostly in H₂ and CO flow rates. Also CO₂ and CH₄ flow rates increased, but to a minor extent. The increase in CH₄ might have been caused by benzene occupying some of the active site for methane reforming. The increase in the open circuit voltage values showed in TABLE II can be compared with the expected voltage increase due to the presence of the tar calculated with equation [1], where R is the universal gas constant, T is the cell operating temperature, F is the Faraday constant and PO_{2anode} the equilibrium oxygen partial pressure at the anode side calculated using the software FactSage. The values measured are in good agreement with the expected ones.

$$\Delta V = V_2 - V_1 = \frac{RT}{4F} * \ln\left(\frac{PO_{2anode1}}{PO_{2anode2}}\right) \quad [1]$$

TABLE II. Outlet gas flowrate (NmL/min) and cell operating voltage measured with different benzene amounts.

	0 g/Nm ³	3 g/Nm ³	6 g/Nm ³	9 g/Nm ³	12 g/Nm ³	15 g/Nm ³
H ₂	231	232	234	239	241	246
CO	97	99	100	104	105	108
CH ₄	9	10	10	10	11	11
CO ₂	152	154	155	154	155	156
Tot.	644	650	655	663	668	677
OCV (V)	0.910	0.911	0.913	0.914	0.915	0.916
ΔV measured (V)	/	0.001	0.003	0.004	0.005	0.006
ΔV calculated (V)	/	0.001	0.002	0.004	0.005	0.006

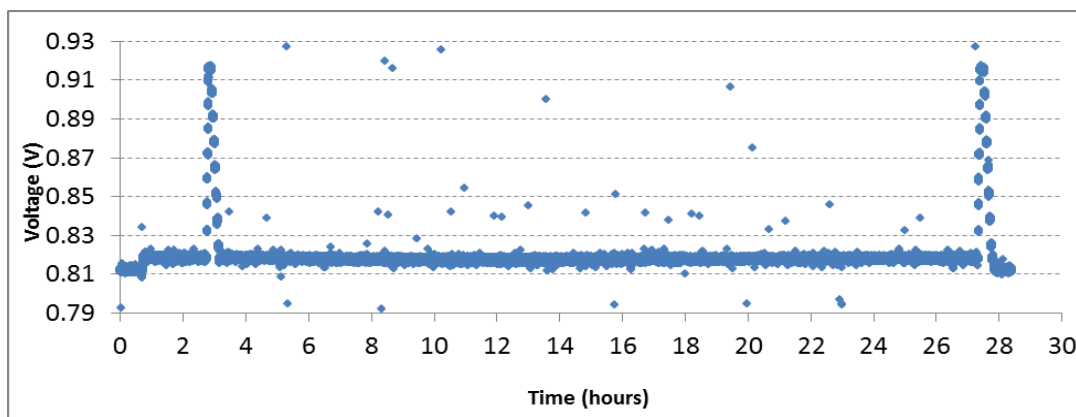


Figure 2. Cell operating voltage over 24 hours period with 15 g/Nm³ benzene.

Naphthalene. The effect of naphthalene was significantly different from that of benzene. In fact, even at low concentrations, the compound appeared to negatively affect the cell catalytic activity. When the tar was introduced, the cell operating voltage slowly dropped and it then reached a stable operating point. When the contaminant was removed, the operating voltage slowly returned to its initial value. The analysis of the outlet gas composition confirmed that this compound seems to behave as a catalyst poison. From the values presented in TABLE II, it appears that naphthalene blocked the active sites for methane reforming and for the reverse water gas shift reaction. In fact, while the flow rates of hydrogen and carbon monoxide decreased, the flows of methane and carbon dioxide increased.

TABLE III. Outlet gas flow rates (NmL/min) and cell operating voltage measured with different benzene amounts.

	0 g/Nm ³	0.2 g/Nm ³	0.7 g/Nm ³
H ₂	223	204	203
CO	95	86	84
CO ₂	10	18	20
CH ₄	152	156	157
Tot.	636	620	621
Operating voltage (V)	0.813	0.804	0.802

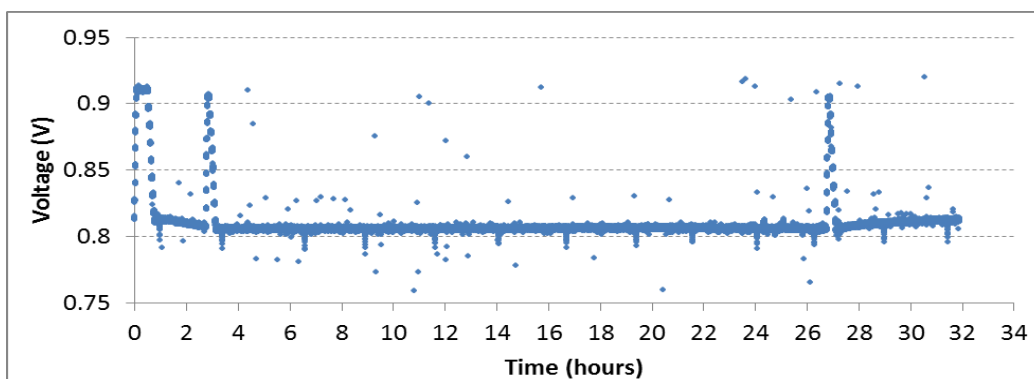


Figure 3. Cell operating voltage over 24 hours period with 0.7 g/Nm^3 naphthalene.

Group 2 experiments

Similar to the tests with benzene, the presence of toluene appeared to increase the amount of fuel available at the anode, and therefore the cell voltage, as visible in Figure 4. The measured OCV was lower than the expected calculated value and the difference increased with increasing toluene content. With all the concentration of toluene tested, there was no noticeable increase in the ASR after the 60 minutes of exposure to the contaminant both in OCV and under current. After keeping the cell under current for 60 minutes, the cell ASR decreased, probably due to a minor increase in the cell temperature. The reforming of toluene was confirmed by the presence of CO , CO_2 and CH_4 , as expected from thermodynamic equilibrium calculations. When HCl was also added, the outlet flow rates of CO_2 and CO decreased. Even low concentrations of HCl seemed to affect the tar reforming, as visible in Figure 4, that shows the ratio between the carbon molar flow rate at the outlet and at the inlet as a function of the HCl concentration when 8.4 g/Nm^3 toluene were present. The inlet carbon molar flow was calculated from the assumed inlet toluene molar flow; the outlet carbon molar flow is the sum of CO , CO_2 and CH_4 molar flows.

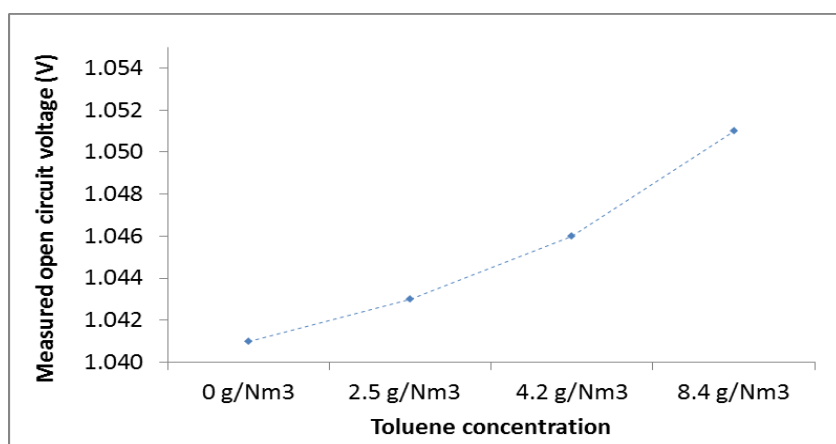


Figure 3. Measured cell open circuit voltage with the different amounts of toluene tested.

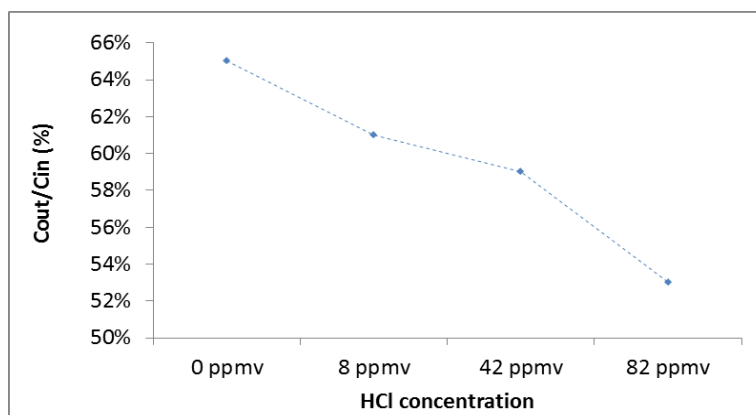


Figure 4. Ratio between the carbon molar flow rate at the cell outlet and at the inlet as a function of HCl concentration.

Group 3 experiments

Similar to the case of benzene and toluene, the presence of acetic acid resulted in an increase in H₂, CO, CO₂ and CH₄ outlet flowrates and, as a consequence, in a higher OCV. When also 0.5 ppmv H₂S were added at the inlet flow, methane reforming seemed completely hindered and WGS partially blocked. The amount of methane at the cell outlet was even higher than the inlet set value. This might indicate that part of the acetic acid underwent thermal decomposition rather than catalytic reforming. Moreover, when 0.5 ppmv H₂S were present and the flow of acetic acid was stopped, there was a clear decrease in the outlet flow rates of H₂, CO and CO₂, thus indicating that sulfur was not affecting the primary tar conversion. Furthermore, tar sampling at the cell outlet did not show the presence of acetic acid or of other compounds when H₂S was present, thus indicating that the primary tar was fully converted. However, a significant amount of carbon was present in the cell inlet ceramic pipe, at the inlet of the ceramic housing, and to a minor extent on the anode surface close to the fuel inlet.

TABLE III. Outlet gas flowrates (NmL/min) and cell open circuit voltage measured when acetic acid and H₂S were fed to the cell.

	Inlet	0 g/Nm ³ 0 ppmv	42 g/Nm ³ 0 ppmv	42 g/Nm ³ 0.5 ppmv	0 g/Nm ³ 0 ppmv
H ₂	150	225	253	168	153
CO	200	116	131	189	156
CH ₄	20	9	12	22	20
CO ₂	150	247	257	190	187
Tot.	150	225	253	168	153
Open circuit voltage (V)		0.904	0.911	0.890	0.884

Conclusion

A series of experiments was performed within the “FlexiFuel-SOFC” project with the aim to determine the possibility to directly reform tar inside the SOFC, and the influence that other biosyngas contaminants (i.e., H₂S and HCl) can have on the process. The results indicate that not all tar compounds might be fed to an SOFC. While benzene and

toluene appeared to be reformed internally, thus being additional fuels for the cell, naphthalene seemed to act as a poison for catalytic reactions, such as methane reforming and reverse water gas shift. Also acetic acid might be regarded as an additional fuel. However, at least part of the acetic acid seemed to undergo thermal decomposition rather than catalytic reforming and it caused severe carbon deposition in the fuel feeding piping and on first parts of the cell anode. The different behavior makes it very important to carefully assess the composition of the tar compounds generated during the gasification process. The presence of the other biosyngas contaminants appeared to have an effect on direct internal tar reforming, even at low concentrations. The tolerance limits should therefore be based on contaminants cross-influence studies and on the expected catalytic reactions occurring in the SOFC. The possibility to directly reform light tar compounds internally is an opportunity for decreasing system complexity. Further studies at cell level with other tar representative compounds are currently on-going at TU Delft laboratories. These test are followed by further investigation at stack level and with biosyngas and real tar compounds from the updraft gasifier. Moreover, high temperature sorbents for H₂S and HCl removal, and catalysts for tar reforming have been tested in lab-scale reactors and in the integrated systems developed within the “FlexiFuel-SOFC” project. These results contributed to the successful design and integration of the biomass gasifier with the SOFC systems.

Acknowledgments

This research was partially supported by the project “FlexiFuel-SOFC”. The project has received funding from the European Union’s Horizon 2020 research and innovation programme under grant agreement No. 641229. The authors acknowledge Marco Graziadio, Roberta Bernardini, Tommaso del Carlo, Marius Kunze and Jiaoyi Wu for the help given in carrying out this work.

References

1. D. Pumiglia et al., *J. Power Sources*, **340**, 150 (2017).
2. M. Liu, M. G. Millan-Agorio, P. V. Aravind, and N. P. Brandon, *J. Electrochem. Soc.*, **158**, B1310 (2011).
3. D. Papurello, A. Lanzini, D. Drago, P. Leone, and M. Santarelli, *Energy*, **95**, 67 (2016).
4. D. Papurello, C. Iafrate, A. Lanzini, and M. Santarelli, *Appl. Energy*, **208**, 637 (2017).
5. T. Namioka, T. Naruse, and R. Yamane, *Int. J. Hydrogen Energy*, **36**, 5581 (2011).
6. H. Madi, S. Diethelm, C. Ludwig, and J. Van herle, *ECS Trans.*, **68**, 2811 (2015).
7. A. Baldinelli, G. Cinti, U. Desideri, and F. Fantozzi, *Energy Convers. Manag.*, **128**, 361 (2016).
8. M. Liu, A. van der Kleij, A. H. M. Verkooijen, and P. V. Aravind, *Appl. Energy*, **108**, 149 (2013).
9. T. S. Doyle, Z. Dehouche, P. V. Aravind, M. Liu, and S. Stankovic, *Int. J. Hydrogen Energy*, **39**, 12083 (2014).
10. D. Papurello, A. Lanzini, P. Leone, and M. Santarelli, *Renew. Energy*, **99**, 747 (2016).
11. M. Hauth, W. Lerch, K. König, and J. Karl, *J. Power Sources*, **196**, 7144 (2011).

12. P. V. Aravind, J. P. Ouweltjes, N. Woudstra, and G. Rietveld, *Electrochem. Solid-State Lett.*, **11**, B24 (2008).
13. J. Mermelstein, N. Brandon, and M. Millan, *Energy and Fuels*, **23**, 5042 (2009).
14. J. Mermelstein, M. Millan, and N. P. Brandon, *Chem. Eng. Sci.*, **64**, 492 (2009).
15. E. Lorente, M. Millan, and N. P. Brandon, *Int. J. Hydrogen Energy*, **37**, 7271 (2012).
16. E. Lorente, C. Berruoco, M. Millan, and N. P. Brandon, *J. Power Sources*, **242**, 824 (2013).
17. P. Hofmann et al., *Int. J. Hydrogen Energy*, **34**, 9203 (2009).
18. P. Hofmann et al., *Int. J. Hydrogen Energy*, **33**, 2834 (2008).
19. F. Fischer, S. Fendt, M. Hauck, C. Lenser, and N. H. Menzler, *Energy Sci. Eng.*, **1** (2019).
20. K. Sasaki et al., *J. Power Sources*, **196**, 9130 (2011).
21. P. Boldrin, M. Millan-Agorio, and N. P. Brandon, *Energy & Fuels*, **29**, 442 (2015).
22. A. Cavalli, M. Kunze, and P. V. Aravind, *Appl. Energy*, **231**, 1 (2018).
23. T. Brunner et al., in *25th European Biomass Conference and Exhibition*,, p. 725–731 (2017).
24. A. Cavalli, R. Bernardini, and P. V. Aravind, in *13th European SOFC & SOE Forum 2018*,, p. 41 (2018).
25. Z. Ud Din and Z. A. Zainal, *Renew. Sustain. Energy Rev.*, **53**, 1356 (2016).
26. N. Trofimenko, M. Kusnezoff, and A. Michaelis, *ECS Trans.*, **78**, 3025 (2017).